 DOI: 10.1002/masy.201000027

Small-Molecule Diffusion in Semicrystalline Polymers as Revealed by Experimental and Simulation Studies

*Fritjof Nilsson, Mikael S. Hedenqvist, Ulf W. Gedde**

Summary: Diffusion of *n*-hexane in poly(ethylene-*co*-1-hexene)s with 15–75 wt.% crystallinity was studied by desorption experiments analyzing data using the Fickian equations with a concentration dependent diffusivity. The effect of the impenetrable crystalline phase on the penetrant diffusivity (D) is described by $D = D_a/(\tau\beta)$, where D_a is the diffusivity of the amorphous polymer, τ is the geometrical impedance factor and β is a factor describing the constraining effect of the crystals on the non-crystalline phase. For a polymer with 75 wt.% crystallinity, $\tau\beta$ varied markedly with penetrant concentration (v_{1a}) in the penetrable phase: 1000 ($v_{1a} = 0$) and 10 ($v_{1a} = 0.15$). This penetrant-uptake had no effect on the gross crystal morphology, i.e. β must be strongly dependent on v_{1a}. Samples saturated in *n*-hexane exhibited a penetrant-induced loosening of the interfacial structure, as revealed by an increase in crystal density that require an increased mobility in the interfacial component and by a decrease in the intensity of the asymmetric X-ray scattering associated with the interfacial component. The geometrical impedance factor has been modelled by mimicking spherulite growth and τ was obtained as the ratio of the diffusivities of the fully amorphous and semicrystalline systems. The maximum τ obtained from these simulations is ca. ten, which suggests that β in the systems with $v_{1a} = 0.15$ takes values close to unity. The simulations showed that the geometrical impedance factor is insensitive to the ratio of the crystal width and the crystal thickness. A free path length scaling parameter characteristic of the amorphous phase correlated with τ.

Keywords: diffusion; morphology; polyethylene; simulation

Introduction

Diffusion of small molecule compounds in semicrystalline polymers is retarded by two different mechanisms. Firstly, the crystals are impenetrable for essentially all common penetrants (helium constitute an exception).[1,2] The penetrant molecule trajectories will be extended in the process of circumventing the crystals. This effect is conveniently accounted for in the geometrical impedance factor (τ), Eq. (1):[3]

$$D = \frac{D_a}{\beta\tau} \quad (1)$$

where D and D_a are the diffusivities of the semicrystalline polymer and the fully amorphous polymer analogue, respectively, and β is the so-called constraining factor. Secondly, the amorphous chain segments are highly constrained originating from their anchoring in the crystals. This retardation is quantified by the β factor, Eq. (1). Even though there is available space for insertion of penetrant molecule segments, the mobility of the polymer chain segments in the proximity of the crystal interface is low causing penetrant caging. We have in a number of papers studied diffusion of *n*-hexane in a wide range of different polyethylenes.[4–13] Polyethylene is an ideal model of crystalline polymers: (i) crystallinity can be varied within a wide range; (ii) the crystal phase changes only moderately over the major part of this crystallinity range; polymers with low crystallinity, however, show coexistent

Fibre and Polymer Technology, School of Chemical Science and Engineering, Royal Institute of Technology, SE-100 44 Stockholm, Sweden
Fax: (+46) 8 208856;
E-mail: gedde@polymer.kth.se

orthorhombic and monoclinic crystal phases;[13,14] (iii) *n*-hexane is highly soluble in the amorphous component and strictly banned from the crystal phase.

Figure 1 displays diffusivity data obtained for a series of poly(ethylene-*co*-1-octene)s covering a wide crystallinity range, 15 to 75 wt.%. The zero concentration diffusivity (D_0) decreases strongly with increasing crystallinity. The amorphous diffusivity (D_a) obtained by extrapolation of the D_0-data to the amorphous density (855 kg m^{-3})[15] is ca. 10^{-6} cm^2 s^{-1}. The product $\tau\beta$ for polyethylene with 75 wt.% crystallinity should thus be close to 1000. The diffusivity at 15 vol.% penetrant concentration in the amorphous phase shows a significantly weaker crystallinity dependence and $\tau\beta$ is only 10 at 75 wt.% crystallinity. It is clear that *n*-hexane sorption at room temperature has no impact on the gross morphology, which means that τ should be the same for diffusion at the two different penetrant concentrations. These data suggest that β has to be very large, at least 100, at infinitely low penetrant concentrations whereas under the more penetrant-rich conditions β attains much lower values (of the order of unity) indicating that the polymer chains near the crystal interface are more mobile and less likely to trap the penetrant molecules. The following two sections of this paper address two related topics: the effect of penetrant on the polymer structure and the dependence of the geometrical impedance factor on crystallinity and crystal shape.

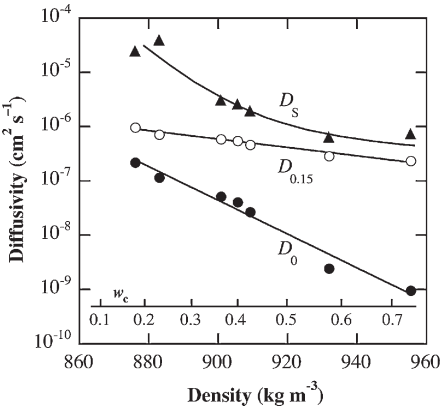

Figure 1.
n-Hexane diffusivity in homogeneous poly(ethylene-*co*-1-octene)s at 296 K as a function of density at 296 K and 101 kPa of pristine polymers and mass crystallinity (w_c): zero-concentration diffusivity (D_0; ●), diffusivity at 15 vol.% *n*-hexane in the non-crystalline component ($D_{0.15}$; ○) and diffusivity at the saturation *n*-hexane concentration (D_s; ▼). The original data are from Neway et al.[7] From Mattozzi et al.[13] with permission from Elsevier, UK.

Structural Changes Accompanying Penetrant Sorption

The structural effects of saturating poly(ethylene-*co*-1-octene)s (crystallinity range: 15–75 wt.%) with *n*-hexane at room temperature were studied by WAXS and Raman spectroscopy.[13] WAXS showed as expected that the intensity of the amorphous halo increased in good agreement with the *n*-hexane uptake and a small shift of the halo peak was recorded consistent with the swelling of the amorphous component.[13]

More unexpected was the contraction of orthorhombic unit cell, which was pronounced for the highly branched polymers (Figure 2a,b). After sorption of deuterated *n*-hexane, the 1415 cm^{-1} Raman band shifted towards lower values indicating a perfection of the orthorhombic crystal phase in accordance with the WAXS data. Hexyl branches being too large to be housed in crystal phase are accumulated in the amorphous phase imposing tensile stresses on the crystal stems expanding the crystal unit cell (Figure 2a,b).[16–18] The observed structural changes, albeit indirect, suggest that the penetrant molecules increases the mobility of the chain segments close to the crystal interface allowing relaxation of the tensile stresses imposed by the amorphous hexyl branches thus leading to densification of the crystal unit cell. A more direct proof of released crystal constraints induced by the solvent uptake is presented in Figure 3. The X-ray diffraction patterns were resolved into Pearson VII scattering peaks (a symmetric distribution function). Asymmetric peaks were revealed on the low 2θ side of both the (200) and (110) orthorhombic

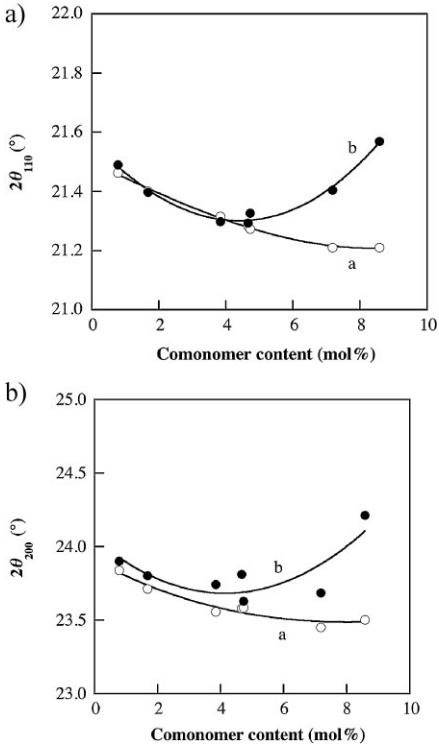

Figure 2.
Scattering angle (2θ) of diffraction peaks corresponding to the following orthorhombic crystal planes: (a) (110): (b) (200), plotted as a function of co-monomer content of polymer. Open symbols represent data taken for the pristine polymers (curve a) and filled symbols represents data for *n*-hexane-saturated samples (curve b). From Mattozzi et al.[13] with permission from Elsevier, UK.

reflections. The two asymmetric peaks (Figure 3) were assigned to an interfacial component in accordance with Baker and Windle.[19] Polymers with a sizeable interfacial peak showed on *n*-hexane sorption a marked reduction in the intensity of the asymmetric peaks (Figure 3). The displayed diffractograms were normalized with respect to the crystalline scattered intensity; it was shown that absolute crystal volume remained constant during sorption.[13]

The orthorhombic crystals remained intact during hexane sorption except for the densification. Hence, there was no increase or decrease in crystal volume in the medium to high crystalline polymers.[13] However, the polymers with the lowest

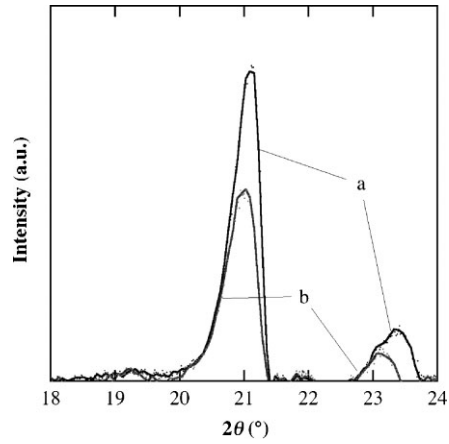

Figure 3.
X-ray scattering associated with the interfacial component for a poly(ethylene-*co*-1-octene) with 1.6 mol% 1-octene: (a) pristine polymer; (b) *n*-hexane saturated polymer. The shown intensities were normalized with respect to the crystalline scattering. From Mattozzi et al.[13] with permission from Elsevier, UK.

crystallinities showed the coexistence of orthorhombic and monoclinic crystal phases. The monoclinic crystal phase showed partial melting on hexane sorption.[13]

Mimicking Spherulite Formation and Simulating Penetrant Diffusion

Spherulite growth was mimicked using an algorithm based on observations made by electron microscopy.[20–23] A detailed description of the method used to build of polyethylene spherulites are provided by Nilsson et al.[12] A brief description follows below. The built spherulite becomes a fully continuous crystal skeleton structure with branching and splaying lamellar bands. The algorithm is using random numbers (Monte Carlo method) with set probabilities for continuous 'linear' growth, i.e. adding a crystal brick and branching. The crystals are inflexible, which means that their growth stops on impingement. The geometry, i.e. the brick aspect ratio (lengths of crystal brick along **c** and **a** axes), the split and splay angles controlling the direction of a branching daughter lamella with respect to mother lamella (Figure 4) and the twisting period, was set to realistic values.

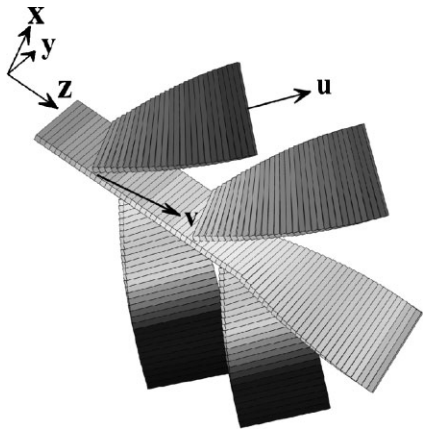

Figure 4.
Early stages of spherulite growth showing basic features of the model: crystal brick, branching features and definitions of split, splay and twisting angles. From Nilsson et al.[12] with permission from Elsevier, UK.

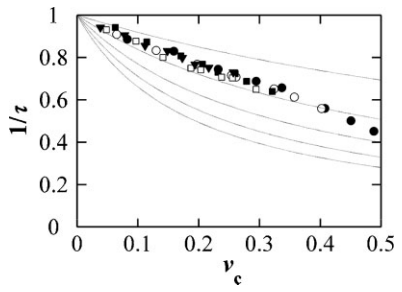

Figure 5.
The reciprocal geometrical impedance factor (τ) as a function of volume crystallinity (v_c) based on the walker statistics obtained during 1.6×10^5 time steps. The jump length was 0.125 lu (length unit, 1 lu = initial crystal thickness). The data were based on simulations carried out on a number of spherulites with splay angle = 22.5°, split angle = 30° and the following crystal aspect ratios: 5 (●), 10 (○), 15 (■), 20 (□), 25 (▼). The corresponding values calculated from the Fricke theory (thin lines) are shown for comparison. From Nilsson et al.[12] with permission from Elsevier, UK.

The simulated spherulite growth occurs as in reality in two stages, the primary growth followed new nucleations onto the existing skeleton by branching in a secondary growth step. The algorithm checked controlled that the crystallinity was uniform in the spherulite; the addition of a layer with a too low or high crystallinity was aborted. Crystal thickening, i.e. growth along the **c**-axis, and crystal widening are also included in the simulation algorithm. Diffusion of penetrant molecules in the built spherulite structure is accomplished by insertion of a 'walker' at an arbitrary point in the amorphous phase. A Monte Carlo method was used to perform a random walk with certain conditions: (i) the walker cannot enter the crystal phase; (ii) different conditions were tested for simulating the movement of a walker reaching the crystal interface. However, the different method used had only a minor impact on the diffusive trajectories.[12] Figure 5 shows that τ is essentially independent of the crystal aspect ratio and only depends on the crystallinity. This counter-intuitive finding, clearly in disagreement with the Fricke theory, called for further analysis. A great number of random points, all located in the amorphous phase, were obtained by a random number method. From each point, a number of free path lengths were obtained; the latter being defined as the distance between the point and the impenetrable crystal face (Figure 6a). All points contributed to the overall free path length distribution from which an average value was determined. The free path length distribution describes the outlook from the penetrant molecules at any time and thus their degree of motion freedom. Figure 6b shows that reciprocal τ scales proportional to the logarithm of the average free path length and again (implicitly) that the latter is essentially independent on the crystal aspect ratio. We have not seen in literature any use of a direct correlation between τ and a geometrical property of the amorphous phase itself. The lack of implication of the crystal aspect ratio on τ can be intuitively understood. Crystals with a high aspect ratio block the diffusion along the lamella normal direction. However, diffusion along **a** is free to the edge of the crystal, which is a relatively long distance in the case of a crystal with high aspect ratio. The two effects are thus counteractive with regard to diffusion.

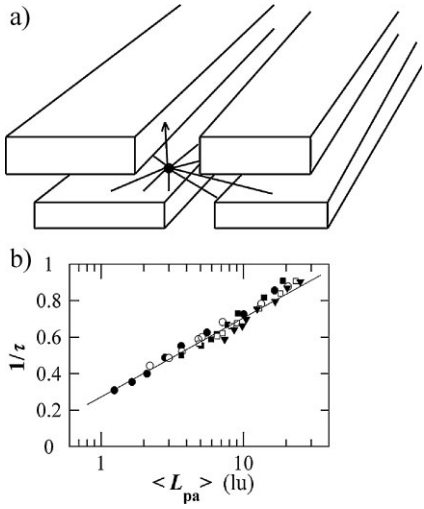

Figure 6.
(a) Sketch illustrating the definition of free path length. (b) Reciprocal of the geometrical impedance factor τ as a function of the average free path length (logarithmic scale) for spherulites with splay angle = 22.5°, split angle = 30° and the following crystal aspect ratios: 5 (●), 10 (◯), 15 (■), 20 (□), 25 (▼). The data presented are based on distributions with free path lengths truncated above 30 lu. From Nilsson et al.[12] with permission from Elsevier, UK.

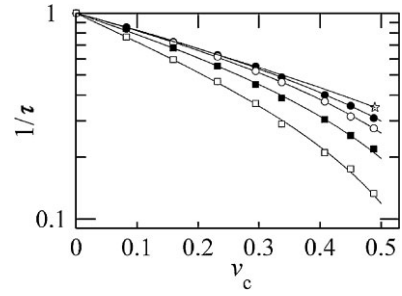

Figure 7.
Reciprocal of the geometrical impedance factor (τ) as a function of volume crystallinity (v_c) based on the walker statistics obtained in a spherulite with crystal aspect ratio = 5, splay angle = 22.5°, split angle = 30°. The jump length was varied: 0.125 lu (●), 0.25 lu (◯), 0.5 lu (■) and 1 lu (□). The uppermost curve (represented by a star) was obtained by extrapolating data to zero jump length. From Nilsson et al.[12] with permission from Elsevier, UK.

Figure 7 shows the effect of jump length on τ. Trajectories based on longer jumps (e.g. 1 lu) experience more hindrance to the motion than trajectories based on shorter jumps: MD simulations reveal jump length of the order of Angstrom.[10] Hence, a more realistic assessment of τ is obtained by extrapolating data to zero jump length (Figure 7). In this case, the data fall on a straight line in the log $\tau - v_c$ diagram, which is exactly the outlook of the experimental data presented in Figure 1.

Figure 8 shows that data obtained by simulation compares well with experimental data, for which the constraining factor is assumed to be small (close to unity). Both the linear character and the order of magnitude of change in τ are comparable.

Building of Crystal Interfaces

In order to generalize the model and to make it immediately applicable to predict diffusivities for semicrystalline polymers a multi-scale approach is required. It is possible to modify the simple mesoscale approach to adapt to the conditions prevailing during zero concentration diffusion simply by trapping (i.e. having a long residence) the walker when it reaches the crystal interface. A more scientifically interesting option would be to build a sandwich based on two crystal lamellae and an amorphous phase in between in order to model diffusion by molecular dynamics simulation. The statistics from

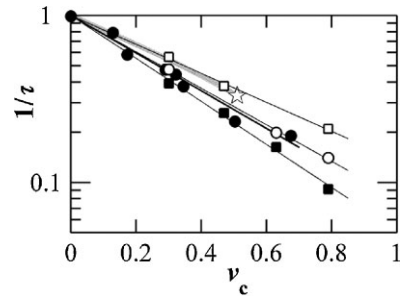

Figure 8.
The reciprocal of the geometrical impedance factor (τ) as a function of volume crystallinity for the different PE's with the following penetrants: *n*-hexane, 15 vol.% in the amorphous component (●),[7,13] CH_4 (◯),[24] N_2 (■),[24] and Ar (□).[24] The latter three sets of data were obtained from permeation data taken at 80 °C at 10 MPa. The line predicted by simulation is displayed as a grey line. From Nilsson et al.[12] with permission from Elsevier, UK.

this simulation would be used as an input in the MC walker simulation. In this section results of preliminary attempt to build the interfacial structure are presented. A Monte-Carlo simulation tool for determining the tie-chain concentration as well as of other relevant structures for stacks of locally parallel polyethylene crystal lamellae was developed. The lamellar stack was build with preset values of crystal thickness (L_c), amorphous thickness (L_a), with periodic boundary conditions and with predefined possible crystal stem positions corresponding to orthorhombic crystal packing. One endpoint of a polymer chain with known chain length was attached to a random empty crystal stem, forcing the chain to progress straight through the crystal layer. Once the chain penetrated the other face of the crystal it could either (with probability p) immediately re-enter the crystal surface on an adjacent empty position or (with probability 1-p) initiate a phantom-chain random walk, which continued walking in the amorphous layer until it touched either of the crystal layers sufficiently close to an empty stem position. A tie-chain is defined as a phantom-chain which starting point and endpoint were positioned on different crystal layers. The procedure was repeated until the whole chain was traversed. New chains were then added until a satisfactory large fraction of the allowed stem positions were filled. The tie-chain concentration (x_{tc}), defined as the number of tie-chains divided by the number of filled stems, and the relative amorphous density ($\rho_{a,rel}$), defined as the amorphous density (ρ_a) divided by the crystalline density (ρ_c), were calculated and were averaged over several simulations.

A first task was to calculate $\rho_{a,rel}$ and x_{tc} as function of filling degree for different values of the probability (p) of adjacent re-entry (Figure 9). This provides an indication of an appropriate filling degree and of reasonable p-values, given that $\rho_{a,rel}$ for polyethylene is ca. 0.85. It was noticed that at low filling fractions (<0.04) too few tie-chains had formed for obtaining reliable

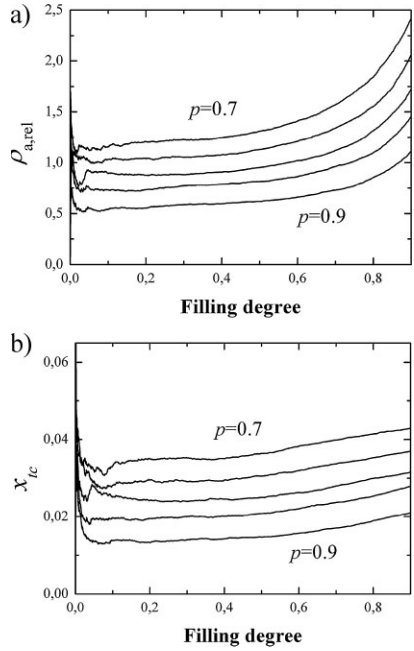

Figure 9.
(a) Relative amorphous density as function of filling degree for the following adjacent re-entry probabilities (p): 0.7 (top) in steps of 0.05 to 0.9 (bottom). (b) Tie-chain concentration as function of filling degree for different p values: 0.7 (top) in steps of 0.05 to 0.9 (bottom). Both diagrams are based on simulations using 100 runs with the following parameter values: $T = 400$ K, chain length = 10 000 carbon atoms, and $L_c = L_a = 10$ nm.

statistics and at high filling degrees (>0.6) the relative amorphous density increased unrealistically due to the limited number of remaining empty crystal stem positions. The lack of available space for attachment extends the amorphous random walk distance. A physically reasonable p-value was 0.8 with a filling of 0.4 resulting in x_{tc} of ca. 2.5%.

A second task was to determine the influence of the chain-length and the crystal thickness on the relative amorphous density and on the tie-chain concentration (Figure 10). The test was performed for molecules with different chain lengths, from 1000 to 128 000 carbon atoms. The calculations were made for a typical HDPE (cystallinity = 67 vol.%, $L_a = 10$ nm and $L_c = 20$ nm) and an LDPE (cystallinity = 50 vol.%, $L_a = 10$ nm and

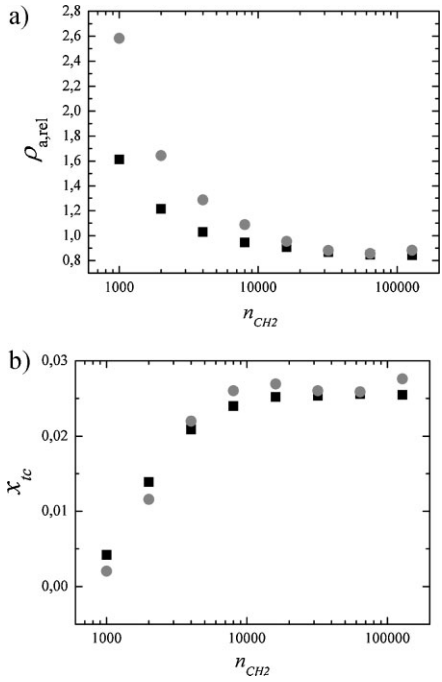

Figure 10.
(a) Relative amorphous density as function of chain length (expressed in number of methylene units). (b) Tie chain concentration as a function of chain length (expressed in number of methylene units). Filled circles: Structures with $L_c = 20$ nm; $L_a = 10$ nm; Filled squares: Structures with $L_c = 10$ nm; $L_a = 10$ nm.

$L_c = 10$ nm). The amorphous density decreased with increasing chain-length and with decreasing crystal thickness due to the condition that no chain-ends were allowed inside the crystals. This effect is artificial; linear molecules of such low molar mass would crystallize without much chain folding resulting in dominantly extended-chain crystals with a very high crystallinity. The tie-chain concentration increased, as expected, with chain-length even though the limited number of stem positions may have had an anomalous effect on the results obtained for the high molar mass systems.

Conclusion

Data for the *n*-hexane diffusivity in polyethylene showing a major decrease in the constraining factor with increasing penetrant concentration have found a structural interpretation using data obtained by WAXS and Raman spectroscopy: the penetrant molecules enters the region close the crystal interface and increases the mobility of the polymer chain segments in this region. This leads to a reduction of trapping of the penetrant molecules and, furthermore, it will allow a denser packing of the stems in the orthorhombic crystals. Simulations of spherulite growth allowing design of polyethylene-like spherulites provide new insight into the structural interpretation of the geometrical impedance factor. A new method has been developed for the characterizing the amorphous phase yielding a scalar paramater (average free path length) that show a unique relationship with the geometrical impedance factor (or the diffusivity). Preliminary results from building crystal-amorphous sandwich structures are presented.

[1] W. R. Vieth, "*Diffusion in and through Polymers*", Hanser Verlag, Munich 1991.
[2] M. Hedenqvist, U. W. Gedde, *Progr. Polym Sci.* **1996**, *21*, 299.
[3] A. S. Michaels, H. J. Bixler, *J. Polym. Sci.* **1961**, *5*, 413.
[4] M. Hedenqvist, A. A. Angelstok, L. Edsberg, P. T. Larsson, U. W. Gedde, *Polymer* **1996**, *37*, 2887.
[5] B. Neway, M. S. Hedenqvist, V. B. F. Mathot, U. W. Gedde, *Polymer* **2001**, *42*, 5307.
[6] B. Neway, M. S. Hedenqvist, U. W. Gedde, *Polymer* **2003**, *44*, 4003.
[7] B. Neway, Å. Westberg, A. Mattozzi, M. S. Hedenqvist, M. Giacinti Bascetti, V. B. F. Mathot, U. W. Gedde, *Polymer* **2004**, *45*, 3913.
[8] A. Mattozzi, B. Neway, M. S. Hedenqvist, U. W. Gedde, *Polymer* **2005**, *46*, 929.
[9] A. Mattozzi, P. Serralunga, M. S. Hedenqvist, U. W. Gedde, *Polymer* **2006**, *47*, 5588.
[10] A. Mattozzi, M. S. Hedenqvist, U. W. Gedde, *Polymer* **2007**, *48*, 5174.
[11] A. Mattozzi, M. Minelli, M. S. Hedenqvist, U. W. Gedde, *Polymer* **2007**, *48*, 2453.
[12] F. Nilsson, U. W. Gedde, M. S. Hedenqvist, *Eur. Polym. J.* **2009**, *45*, 3409.
[13] A. Mattozzi, P. T. Larsson, M. S. Hedenqvist, U. W. Gedde, *Eur. Polym. J.* **2010**, *46*, 381.

[14] J. L. Pezzutti, R. S. Porter, *J. Appl. Polym. Sci.* **1985**, *30*, 4251.
[15] G. Allen, G. Gee, G. J. Wilson, *Polymer* **1960**, *1*, 456.
[16] P. R. Howard, B. Crist, *J. Polym. Sci., Polym. Phys. Ed.*, **1989**, *27*, 2269.
[17] A. M. E. Baker, A. H. Windle, *Polymer* **2001**, *42*, 651.
[18] S. Rabiej, *Eur. Polym. J.* **2005**, *41*, 393.
[19] A. M. E. Baker, A. H. Windle, *Polymer* **2001**, *42*, 667.
[20] D. C. Bassett, R. H. Olley, *Polymer* **1985**, *25*, 935.
[21] D. C. Bassett, A. S. Vaughan, *Polymer* **1986**, *26*, 717.
[22] D. C. Bassett, R. H. Olley, I. A. M. al Rehail, *Polymer* **1988**, *29*, 1539.
[23] U. W. Gedde, A. Mattozzi, *Adv. Polym. Sci.* **2004**, *169*, 29.
[24] B. Flaconnéche, J. Martin, M. H. Klopffer, *Oil & Gas Sci. Techn.* **2001**, *56*, 261.

